

## **Vehicle Maneuvering-style Recognition in identifying the Culprit for a Road Accident**

**Muhammad Shoaib Siddiqui**

Faculty of Computer & Information Systems, Islamic University of Madinah, Kingdom of Saudi Arabia

shoaib@iu.edu.sa

**Abstract:** One of main reasons of road-side accidents (RSA) is the reckless by the driver. Reckless drivers induce danger on the road and their surroundings, which could result in deadly accidents both on road and off the road. High acceleration, frequent lane changes, lane changing in high speed, turning at high speed, and braking late or suddenly are some of the activities by drivers that cause these deadly accidents. In this paper, we have proposed and developed a driving style recognition system, which would alert the driver to drive safely. It would also help in identifying the driver at mistake during a road-side accident. In this paper, we have gathered data from an accelerometer and a gyroscope to recognize the vehicle maneuvering style of the driver. We have applied and compared the results of two well-known classifiers, i.e. Support Vector Machine (SVM) and K-Nearest Neighbor (KNN) to identify the driving activity. We have also explored different features extraction techniques to identify the best solution. After, the driving activity is recognized, it is further classified to detect the driving style, as reckless or adequate. Later on, the system can generate alarm to the driver through an actuator and use a weight-based algorithm to identify the driver at fault, based on the driving style, in case of a RSA.

**Keywords:** maneuvering style; road-side accident, classification; feature extraction; driving style; driving activity.

## التعرف على أسلوب مناورة السيارة في تحديد الجاني لحادث سير

**الملخص:** أحد الأسباب الرئيسية للحوادث المرورية (ر س ا) هو التهور من قبل السائق. السائقون المتهورون يشكلون خطراً على الطريق ومحيطهم، مما قد يؤدي إلى حوادث مميتة سواء على الطريق أو خارجه. تعد بعض التصرفات التي يقوم بها السائقون؛ كالسرعة العالية، والتغيرات المتكررة في المسار، وتغيير المسار في السرعة العالية، والانعطاف بسرعة عالية، والكبح في وقت متأخر أو فجأة، سببا في هذه الحوادث المميتة. في هذه الورقة اقترحنا وطورنا نظام التعرف على نمط القيادة، والذي من شأنه تنبيه السائق إلى القيادة بأمان. كما أنه سيساعد في التعرف على السائق المخطيء أثناء حادث على جانب الطريق. في هذا المقال قمنا باقتراح وتطوير نظام تعرف على طريقة السياقة والذي سينبه السائق للسياقة بحذر. وسيساعد كذلك على تحديد السائق المخطيء خلال حادث مروري. في هذا المقال قمنا بجمع البيانات من مقياس التسارع وجيروسكوب للتعرف على أسلوب السياقة لدى السائق. قمنا بتطبيق ومقارنة نتائج لمصنفين معروفين جدا، لمعرفة دعم ناقلات الجهاز (س ف م) والجار الأقرب-ك (ك ن ن) لتحديد نشاط القيادة. لقد استكشفنا أيضاً عدة تقنيات لاستخلاص ميزات مختلفة من أجل تحديد أفضل الحلول. بعد أن يتم التعرف على نشاط القيادة، يتم تصنيفه أيضاً لاكتشاف نمط القيادة، باعتباره متهوراً أو كاف. في وقت لاحق، يمكن للنظام توليد إنذار للسائق من خلال مشغل، واستخدام خوارزمية تركز على الوزن لتحديد السائق المخطيء، استنادا إلى نمط القيادة، في حالة وجود ر س ا.

### 1. Introduction

With the increasing rate of vehicles on the road, the frequency of road accidents is increasing. In a country like the Kingdom of Saudi Arabia, the rate is relatively higher. Every year more than five hundred thousand road accident are reported and it is estimated that there are almost 7 million vehicles registered in the Kingdom [1]. According to a trend analytical survey, a warning has been reported that if the safety of the road is not ensured and public is not educated, the amount of accident would pass the value of four million till 2030 [2]. Numerous studies have been performed which identify the various causes of these accidents, such as, distractions, sleep, negative emotions, failure to see or observe, awareness, etc. [3]. According to [4], “The Secretary General of the Shura Council declared that the Kingdom has spent on an average 26 billion riyals annually

on car accidents”. According to the data from the Ministry of Interior, General Directorate of Traffic, there were around six hundred thousand accident in the year 2012 [5]. The trend of increase in the number of accident is given in Figure 1. Although the official data are available till 2012; however, the researchers have predicted that the value would increase to four million till 2030 [2].

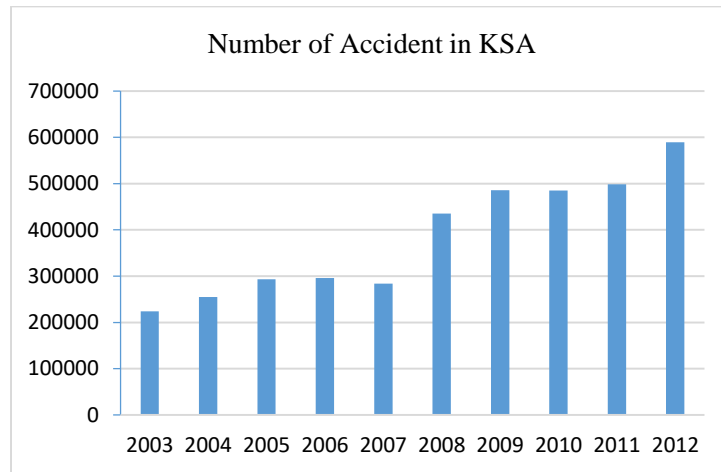


Figure 1: Number of accident in KSA reported (according to the Ministry of Interior - General Directorate of Traffic | Saudi Open Data) [5]

According to the World Health Organization (WHO), about 1.35 million people die every year worldwide, due to road side accidents, while 20.5 million suffer severe trauma. Most of the victims require costly treatments over a long period of time. Along with trauma and suffering, road accidents cause enormous social and economic losses, absorbing 1-3% of the national gross domestic product [29]. Many consequences of a traffic accident can be effectively prevented. However, this requires continuing efforts to develop new methods and programs aimed at improving road traffic safety. The WHO predicted that about 1.9 million people would die each year before 2020 due to road traffic accidents without proper action [30].

Road side accidents (RSA) can be classified as driver-based, infrastructure based, and vehicle based. By providing better road infrastructure, infrastructure traffic accidents can be reduced. Vehicle-based road accidents are caused by defective or outdated vehicles on the road. The governments apply strict rules to vehicle health monitoring and penalties to reduce the number of accidents. Likewise, in the case of driver-based accidents, the authorities imposed heavy fines to prevent reckless and dangerous driving. However, it is a difficult task to check for recklessness and correctly display faulty drivers. Driver based accident are due to over-speeding, reckless

driving, and breaking road rules. In [6], we have proposed a system which can help in identifying the driver at fault in a RSA; however, in this paper, we provide the details of vehicle maneuvering-style recognition system in identifying the culprit for a road accident. The proposed system uses the data gathered from the accelerometer and a gyroscope fitted inside the vehicle and apply pattern recognition mechanism to classify the maneuvering style of the driver. The maneuvering styles are classified as, ‘over-cautious’, ‘normal’, ‘aggressive’, and ‘reckless’.

## **2. Related Work**

Accelerometer is a device which can recognize the change in velocity of a body. A tri-accelerometer gives value for change in velocity in terms of x-axis, y-axis, and z-axis. However, a gyroscope provides the values in x-axis, y-axis, and z-axis for the angular velocity.

There has been many application of accelerometer and gyroscope sensors, such as, human activity recognition [7], fall detection [8], remote subject monitoring in old houses and clinics [9], step counting [10], vehicle path tracking [11], and vehicle maneuvering detection [12].

Most of the proposed systems for human activity recognition use the tri-accelerometer with either a specialized wearable sensor [13] or sensor available inside the smart-phones [14]. The data is gathered from the sensors and feature extraction and classification algorithms are applied on that data to identify the activity being performed by the subject [15] [14]. Classifiers, such as, decision tree, support vector machines, k-nearest neighbor, naïve Bayes, decision table, random forest, etc. have been applied by the researchers to devise an optimal solution for human activity recognition [16]. Similarly, the use of accelerometer is explored in other applications, such as, fall detection [8], remote subject monitoring in old houses [9], and step counting [10].

Some researchers have applied classification mechanism on data gathered from an accelerometer (or in a smartphone) to identify the transportation mode of the subject [11] [17]. The modes could be classified as, in a car, in a train, in a plane, or motor based and non-motor based [11]. Some vehicle tracking and prediction systems have also used the data from accelerometer and other sensors [17]. Furthermore, driver profiling mechanisms are also proposed which use similar techniques [18] [19].

Vehicle maneuvering detection is relatively a less explored area, in which few solution have been proposed which use the data gathered from an accelerometer. Cervantes-Villanueva et al. [12] have

proposed a solution that detects the maneuvering relative to the kinematic state of the vehicle. They have devised a low-computational solution that can be implemented on a smart-phones, which can be used to gather data through their embedded accelerometer and run classification algorithm to detect the vehicle current maneuver as parked, driving, parking, and stopped.

In [28], the authors have presented a driver behavior detection mechanism using a motion sensor/accelerometer. It uses deep learning technology to learn the sample data collected by the sensor deployed in a vehicle. To solve the problem of small sample size and easy overfitting, they have proposed a joint data augmentation (JDA) scheme and designed a new multi-view convolutional neural network model (MV-CNN). MV-CNN and JDA have better generalization ability, reduce the training variance and deviation, and increase the stability of the model training process.

Our work is quite different to the work done by the other researchers presented above. The target of our research is to identify the driver who caused an accident. To identify if the current driver is at fault, we classify the drivers' driving style based on the vehicle maneuvering. For classifying the maneuvering style of the driver, first we need to identify the driving activity, i.e. right-turn, left-turn, lane-change (left and right), braking, and acceleration, and then classify these activities as 'over-cautious', 'normal', 'aggressive', and 'reckless'. As we performed the experiments, we identify that some of these activities are not recognized with higher accuracy based on accelerometer data. Therefore, we have used the data from the gyroscope also. After including the data from gyroscope the accuracy in detecting the driving activities increases as shown in the results section.

We have used two classification techniques i.e. support vector machine (SVM) [20] and K-nearest neighbor (KNN) [21] and compared the results for optimal solution. Similarly, for features extraction, we have used kernel discriminant analysis (KDA) [22], and linear discriminant analysis (LDA) [25] and autoregressive model [24].

The rest of the paper is articulated as follows. Section 3 provides the details of the proposed system and discusses the model. Section 4 provides the experimentation results. Section 5 concludes the paper.

### 3. Vehicle Maneuvering Detection Methods

The proposed vehicle maneuvering detection system is modelled in Figure 2. A node with an accelerometer and gyroscope is mounted inside the vehicle, through which the data is gathered. There are three main modules in the system. The first module is training module, which is used to collect data for the training of the classifiers and calculating model parameters. The second module is the detection module which perceives the driving activity. The third module is for categorizing the activity as adequate or reckless. The details of the model are discussed in the following subsection.

#### 3.1 Data Collection

A MotionNode with a triaxial accelerometer and a gyroscope is used to collect data at 1000 Hz sampling rate. The data from accelerometer shows the change in velocity in x, y, and z directions after every 10 milliseconds, while the data from gyroscope shows the value of angular velocity's x, y, and z components. The data stream is continuously recorded for 1 minutes sample for training scenario created in simulated environment with ideal infrastructure and vehicle conditions. Further specification of data collection is given in the simulation section 4, "Experiments and Results".

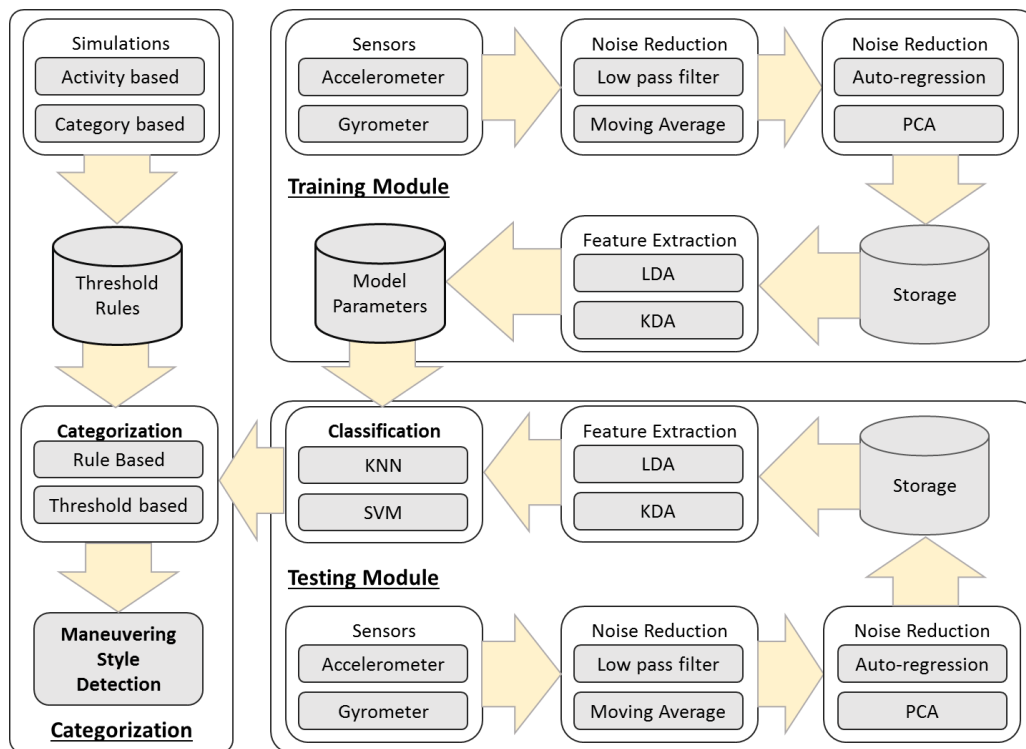


Figure 2. The system model of the proposed driving activity recognition

### 3.2 Noise Reduction

MotionNode [25] accelerometer and gyroscope have noise density of  $50 \mu\text{g}/\sqrt{\text{Hz}}$  (at 2 g range) and 0.1 degrees/second, respectively. There is some noise due to the flexibility of the fiber of which the device is mounted inside the vehicle also. To reduce the noise, we have applied a low pass filter to remove the higher frequencies. As we are using sampling frequency  $F_s=1000$  Hz, we devise out low pass filter with cut-off frequency  $f_0=100$  Hz, and used a second order Butterworth filter, with pre-warping. We have used the Butterworth filter as it rolls off more slowly around the cutoff frequency than the Chebyshev filter or the Elliptic filter, but without ripple [27]. We have also applied the moving average algorithm with order three (3) to smooth the signal. A moving average filter smooths data by replacing each data point with the average of the neighboring data points defined within a given span. The Eq. (1) gives the moving average equation that is used with the value of  $\alpha = 0.3$ .

$$\vartheta_n = \alpha(\vartheta_m) + (1 - \alpha)\vartheta_{n-1} \quad (1)$$

Where  $\vartheta_m$  is the new value and  $\vartheta_n$  is the moving average. Figure 3 shows the effect of noise reduction on the collected data after remove high frequencies and applying moving average.

### 3.3 Feature Extraction

#### Segmentation

After the noise is reduced from the data, we apply segmentation to create segments of data called windows for applying feature extraction on each window. As our data is not tagged with events, we have applied sliding window technique for segmentation. Although this puts a lot of load on computation resources; however, for real-time systems, this is the best option as compared to event-based windows and activity-defined windows. We have used a single window length of 90 samples, which we have identified as optimal after using different window sizes.

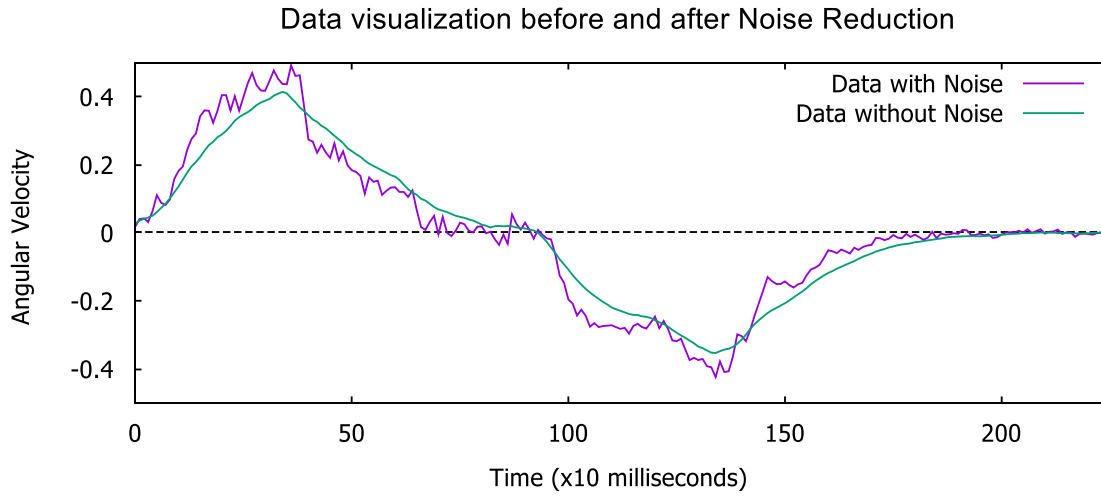


Figure 3. Data from gyroscope for aggressive left-turn, then a right-turn: before noise reduction and after noise reduction applied.

#### Autoregressive Coefficients (AR):

As per related works [7], we have used AR modeling for the gyroscope data. The representation of the AR model is given as Eq. (2)

$$X_n = \sum_{i=1}^m \delta_i X_{n-i} + \varepsilon_n \quad (2)$$

Where,  $X_n$  is the current value of the gyroscope data.  $\delta_1, \delta_2, \dots, \delta_m$  are weighting coefficients for gyroscope,  $m$  is the model order indication the number of the past values used to predict the current value and  $\varepsilon_n$  is the Gaussian white noise.

#### Principal Component Analysis

The data from the accelerometer shows the change in velocity relative to the current position of the body, but it also contains the component of earth gravitational acceleration. To eliminate the gravitational effect, the acceleration of earth coordinate system can be projected in the direction of the vehicle movement. The direction of the vehicle movement would have the largest variance of acceleration. This component can be separated using the PCA algorithm as the first principal in PCA would be the direction of the vehicle [23].

Assume that  $\vartheta_x = (\vartheta_x^1, \vartheta_x^2, \dots, \vartheta_x^m)^T$ ,  $\vartheta_y = (\vartheta_y^1, \vartheta_y^2, \dots, \vartheta_y^m)^T$ , and  $\vartheta_z = (\vartheta_z^1, \vartheta_z^2, \dots, \vartheta_z^m)^T$  represent the x-axis, y-axis, and z-axis accelerations of earth coordinate system. The combination of the x, y, and z, axis data would result in a matrix,  $\mathbf{M} \in \mathbf{R}^{m \times 3}$



$$\mathbf{M} = \begin{bmatrix} \vartheta_x^1 & \vartheta_y^1 & \vartheta_z^1 \\ \vartheta_x^2 & \vartheta_y^2 & \vartheta_z^2 \\ \vdots & \vdots & \vdots \\ \vartheta_x^m & \vartheta_y^m & \vartheta_z^m \end{bmatrix} \quad (3)$$

Then the covariance matrix  $\Gamma$  can be calculated as,

$$\Gamma = \frac{1}{m} (\mathbf{M} - E(\mathbf{M}))(\mathbf{M} - E(\mathbf{M}))^T \quad (4)$$

Where  $E(\mathbf{M})$  is the expectation operation for each column of matrix  $\mathbf{M}$ .  $\Gamma$  can be diagonalized as it is symmetric matrix:

$$\Gamma = \mathbf{\Omega}\mathbf{\Lambda}\mathbf{\Omega}^T \quad (5)$$

Where  $\mathbf{\Omega}$  and  $\mathbf{\Lambda}$  are eigenvector and eigenvalue matrices of  $\Gamma$ , respectively. After ranking the eigenvalue in descending order and reconstructing the eigenvector matrix corresponding to eigenvalues, a new matrix  $\tilde{\mathbf{Q}}$  is obtained. The transformation matrix for PCA can be represented as;

$$\mathbf{P} = \tilde{\mathbf{Q}}^T \quad (6)$$

The final PCA transformation is:

$$\mathbf{G} = \mathbf{P}\mathbf{M}^T \quad (7)$$

Where the first row of the matrix  $\mathbf{G}$  is the first principal component, i.e. our transformed data.

### LDA and KDA

The goal of LDA [26] is to find a projection which gives the maximum class separation. It tries to find the vector in the underlying space that gives the best discrimination amongst different classes. LDA uses Eq. (8) and Eq. (9) for calculating within  $S_W$ , and between  $S_B$  class comparison, respectively [26].

$$S_B = \sum_{i=1}^k J_i (\bar{m}_i - \bar{m})(\bar{m}_i - \bar{m})^T \quad (8)$$

$$S_W = \sum_{i=1}^k \sum_{m_s \in C_i} (m_s - \bar{m}_i)(m_s - \bar{m}_i)^T \quad (9)$$

Where,  $J_i$  is the number of vectors in  $i^{th}$  class  $C$ .  $k$  is the number of classes, which in this case is the number of driving activities.  $\bar{m}_i$  is the mean of vectors in class  $C$  while, and  $\bar{m}$  represents the mean of all the vectors.

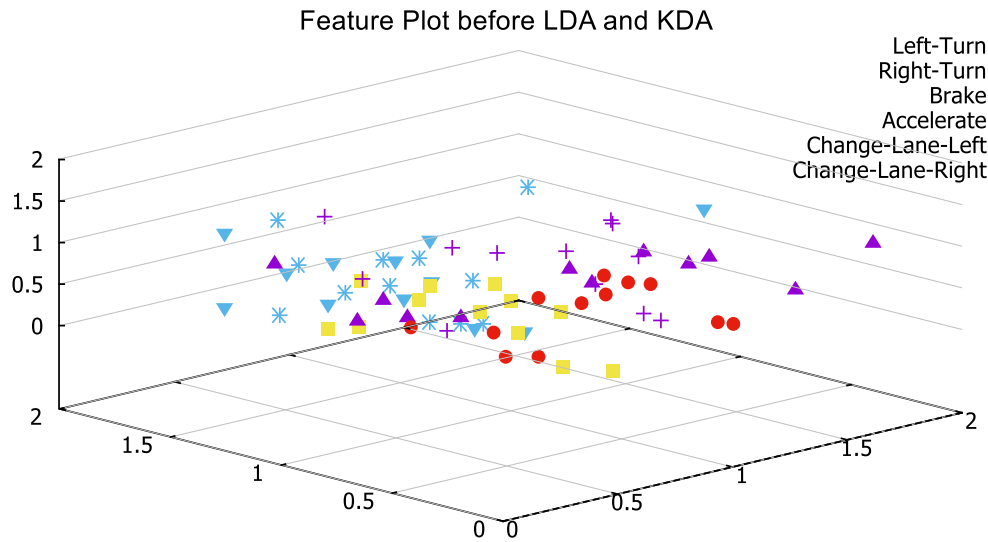


Figure 4. Feature plot for the six activities before discriminant analysis is performed showing high-in and low between class variances.

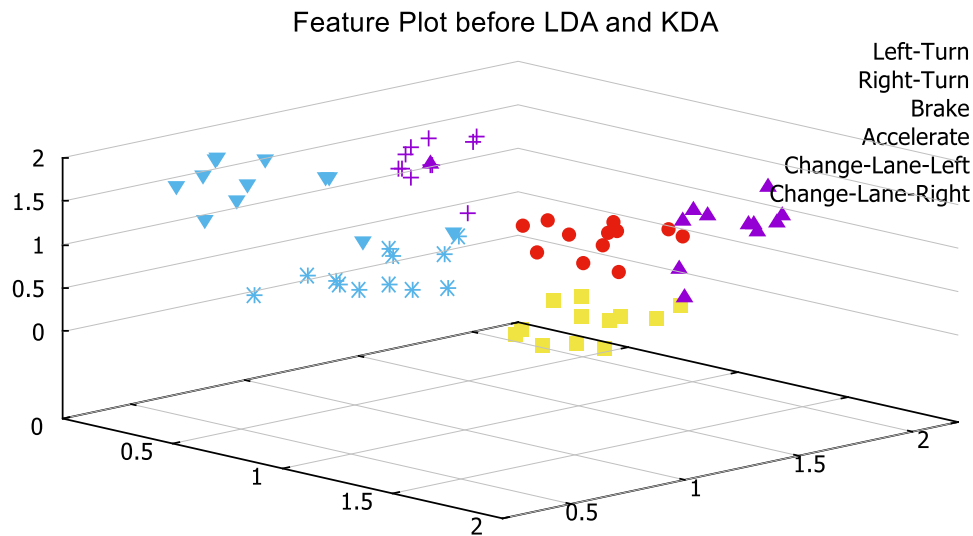


Figure 5. Feature plot for the six activities after KDA showing low-in and low between class variances

To extend LDA to non-linear mappings, the data, given as  $l$  points  $\vartheta_i$  can be mapped to a new feature space,  $F$ , via some function  $\varphi$ . However this mapping is computationally heavy. Therefore, the data can be implicitly embedded by rewriting the algorithm in terms of dot products and using the kernel trick in which the dot product in the new feature space is replaced by a kernel function. As proved by [7], Eq. (8) is equivalent to Eq.(10);

$$J(\vartheta) = \frac{\vartheta^T \mathbf{K} \mathbf{W} \mathbf{K} \vartheta}{\vartheta^T \mathbf{K} \mathbf{K} \vartheta} \quad (10)$$

Where  $\vartheta = [\vartheta_1, \vartheta_2, \dots, \vartheta_m]^T$  are the coefficients, and their optimal values are given by the eigenvectors with respect to the maximum values of:

$$\mathbf{K} \mathbf{W} \mathbf{K} \vartheta = \lambda \mathbf{K} \mathbf{K} \vartheta \quad (11)$$

Where  $\mathbf{K}$  is the kernel matrix ( $\mathbf{K}_{ij} = \mathbf{K}(x_i, x_j)$ ) and  $\mathbf{W}$  is defined as:

$$W_{ij} = \begin{cases} \frac{1}{m_k}, & \text{if } x_i \text{ and } x_j \text{ belongs to } k^{\text{th}} \text{ class} \\ 0, & \text{otherwise} \end{cases} \quad (12)$$

For a new pattern  $z$ , its projection onto KDA basis vector  $\omega$  in  $F$  is calculated as:

$$(\omega, \varphi(z)) = \vartheta^T \mathbf{K}(:, z) \quad (13)$$

Where,

$$\mathbf{K}(:, z) = [K(z_1, z), \dots, K(z_m, z)]^T \quad (14)$$

Figure 4 shows the feature set before applying the discriminant analysis where the features have high-in and low between class variances, while Figure 5 shows the feature plot after the application of KDA has reduced the variance.

The reason for using discriminant analysis is to establish a significant difference in the classes of data which helps in improving the accuracy of the classification algorithm. LDA and KDA are two of the most famous algorithms used for this purpose. LDA is capable of finding only linear mapping, hence the results of feature extraction are not good as our data does not have linear boundaries. KDA applies non-linear mapping; therefore, it provides better feature extraction but creates extra features sets. Therefore, to attain the advantages of both and obtain best results, we have applied LDA on our data first and then applied KDA to further enhance the feature extraction phase. The result can be seen in Figure 5.

### 3.4 Classification

We have considered the driving maneuver activities as, (1) right-turn, (2) left-turn, (3) brake, (4) accelerate, (5) right-lane-change, and (6) left-lane-change. We have experimented with two classifiers, i.e. k-nearest neighbor, and support vector machines.

### **K-Nearest Neighbor (KNN)**

K-Nearest Neighbor is a non-parametric classification algorithm in machine learning abundantly used in activity recognition [21]. During the training phase, the features extracted using the LDA and KDA algorithms are provided to the KNN, which are vectors in three dimensional feature space, each with a class label, such as, right-turn, left-turn, brake, accelerate, right-lane-change, and left-lane-change. For training of one class of activity the accelerometer data and the data from the gyroscope are separately forwarded to the classifier and also together. Hence, we have three set of classification based on the input data, called A for accelerometer only, G for gyroscope only, and C for both accelerometer and gyroscope. The feature vectors and class labels are stored as model parameters during the training phase. Euclidian distance is used as the measure of distance metric, while the value of  $k=1$  is used in our experimentation.

### **Support Vector Machine (SVM)**

SVM is a supervised classification mechanism used in pattern recognition to classify featured data using hyperplanes [20]. We have used one-against-one approach to build and decompose our multiclass classifier as multiple binary classifiers. Training data is created for each class of activity. After noise reduction, auto-regression, the extracted feature-set from the accelerometer and gyroscope is passed to the SVM which builds a model that assigns new examples to one activity or the other, making it a non-probabilistic binary linear classifier. The class of data is pre-defined during the training phase. During the testing/detection phase, as the class is not pre-defined, the supervised learning is not possible. A Gaussian kernel approach is used to devise a non-linear SVM in our experimentation.

### **3.5 Maneuvering Style Detection**

After the activity is classified as either a right-turn, a left-turn, a brake, an accelerate, a right-lane-change, or a left-lane-change, the maneuvering style detection is performed to categorize the maneuvering style as ‘over-cautious’, ‘normal’, ‘aggressive’, and ‘reckless’.

Table 1. Threshold variance value for vehicle maneuvering-style detection

Driving Activity	Maneuvering Style			
	Over-cautious	Normal	Aggressive	Reckless

Left-turn	$0.0 \leq g \leq 0.05$	$0.05 \leq x \leq 0.20$	$0.21 \leq x \leq 0.45$	$x \geq 0.46$
Right-turn	$0.0 \leq g \leq 0.05$	$0.05 \leq x \leq 0.20$	$0.21 \leq x \leq 0.45$	$x \geq 0.46$
Brake	$0.0 \leq a \leq 0.05$	$0.05 \leq a \leq 0.20$	$0.21 \leq a \leq 0.5$	$a \geq 0.5$
Accelerate	$0.0 \leq a \leq 0.05$	$0.05 \leq a \leq 0.24$	$0.25 \leq a \leq 0.44$	$a \geq 0.45$
Lane-change-left	$0.0 \leq g \leq 0.05$	$0.05 \leq g \leq 0.10$	$0.11 \leq g \leq 0.4$	$g \geq 0.4$
Lane-change-right	$0.0 \leq g \leq 0.05$	$0.05 \leq g \leq 0.10$	$0.11 \leq g \leq 0.4$	$g \geq 0.4$

We have used a rule-based approach in categorizing the maneuvering style of the driver which is based on the statistical analysis of the data for the concerned activity. For example, if the driving activity is classified as a left turn, then we define the threshold values for the variance of the data (y-axis) as: 0 - 0.05 as over-cautious, 0.05 – 0.2 as normal, 0.2 – 0.45 aggressive, and greater than 0.45 to be reckless. The values for the other driving activities are given in Table 1. In the simulated environment, as discussed before, certain scenarios were artificially created according to the different driving styles for each driving activity. For example, for activity ‘left-turn’, over-cautious (too slow) left turn was performed which gave very small value in G-force (less than 0.05). Similarly, many ‘normal’ left-turns were performed to identify the range of G-force values for non-aggressive left-turn. After that the same simulations are performed to identify the range of G-force for aggressive and reckless classification. These threshold values are calculated after 15 simulations for each category of each driving activity. After visualizing the simulated data, the threshold values were calculated by the author. For activities, right-turn, left-turn, right-lane-change, and left-lane-change, y-axis values from the gyroscope are used, while for activities brake and accelerate, z-axis values from accelerometer are used.

## 4. Experiments and Results

### 4.1 Data Collection

We have used a MotionNode, a miniature 3-DOF inertial measurement unit (IMU), which includes triaxial accelerometer, gyroscope, and magnetometer for use in motion sensing applications [25]. The device is 35 x 35 x 15 mm in size, shown in Figure 6, with orientation output of 3-DOF with full 360 degrees range in all three axes. The tri-accelerometer can measure linear acceleration in the range of  $2\pm g$  or  $6\pm g$  with resolution  $190 \mu g \pm 5\%$  (at 2 g range). The gyroscope can measure

angular velocity with range  $\pm 2000$  degrees/second and resolution 0.07 degrees/second. The device is mounted inside the car on the fiber dashboard in a Toyota Camry 2011 for data collection. The data is gathered are the sampling rate of 1000 Hz.



Figure 6. MotionNode device which includes an accelerometer, a gyroscope and a magnetometer.

## **4.2 Experimentation Setup**

For the learning/training phase eight simulated scenarios are recorded for each category of each driving activity. Four simulated scenarios are recorded for testing phase for each category in each activity also. Given that there are six activities and four categories,  $6 \times 4 \times (8 + 4) = 288$  simulated scenarios are recorded. Four new simulated scenarios and four simulated scenarios from the training phase are used to check the accuracy of the classifiers. Hence, for each driving activity, thirty-two simulated test cases are used for learning and thirty-two cases are used for testing accuracy, out of which sixteen are included in the training.

## **4.3 Results & Discussion**

We have performed the experiments with different settings to evaluate the feature extraction and classification algorithms. We have experimented without using LDA and KDA (no-DA), using LDA, and using KDA for features extraction. Similarly, we have evaluated with KNN and SVM separately. Furthermore, we have evaluated the mechanism on accelerometer data only, gyroscope data only, and on data from both the sensors.

Figure 7 shows the results for different classifiers and features extraction techniques on accelerometer data only. Figure 8 shows the results for different classifiers and features extraction techniques on gyroscope data only. Figure 9 shows the results for different classifiers and features

extraction techniques on both gyroscope and accelerometer data. As shown by the results, without applying discriminant analysis, the results are very poor. This is because the variance in the features is very high and the classes have no distinct boundaries. After the application of LDA, the accuracy improves but it is less than the accuracy of the KDA. This is due to the fact that LDA is linear, while KDA is a non-linear discriminant analyzer.

For the classifiers, we have observed that SVM performs better than the KNN, although the value for  $k$  used is one (1). From the literature review it is also confirmed that for activity recognition, SVM has better classification accuracy than the KNN.

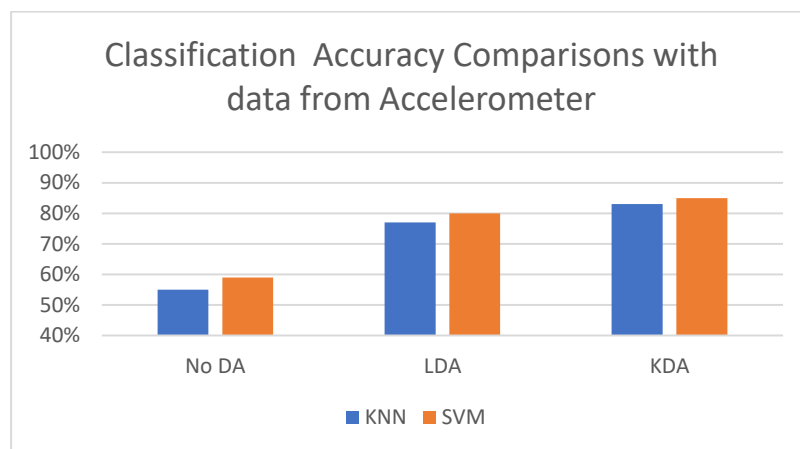


Figure 7. Driving activity classification accuracy for classifiers KNN and SVM for features extraction techniques on accelerometer data only

After the driving activities have been classified and detected, we perform further classification to categorize the activities as ‘over cautious’, ‘normal’, ‘aggressive’, and reckless. As discussed in section 3, we have applied a rules based approach in categorizing the activities. Table 2 shows the accuracy chart for the driving style classifications. Accuracy shows the driving style is correctly categorized, while the false positive is when a style is detected but that is not the case. The lower values of accuracy for the ‘over-cautious’ is due to the negligible change in the values of accelerometer and gyroscope due to the noise reduction scheme which make the signal smooth and removes the higher frequencies. The normal driving style of the driver becomes similar to the over-cautious style; hence, the high false positive rate.

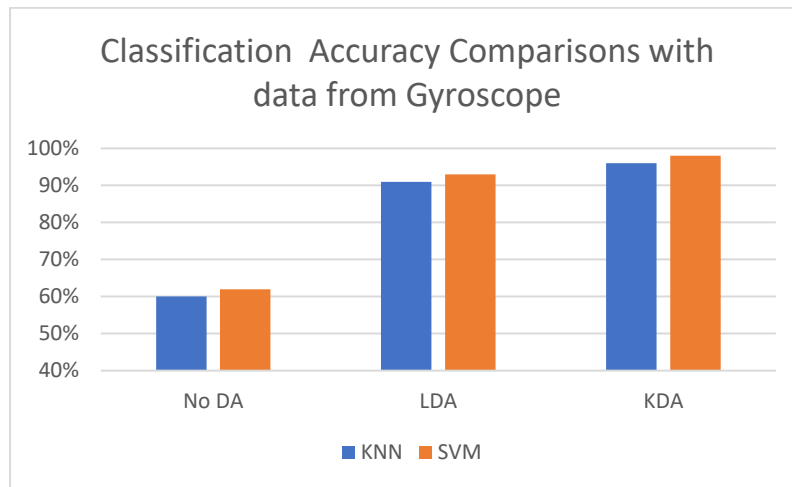


Figure 8. Driving activity classification accuracy for classifiers KNN and SVM for features extraction techniques on gyroscope data only

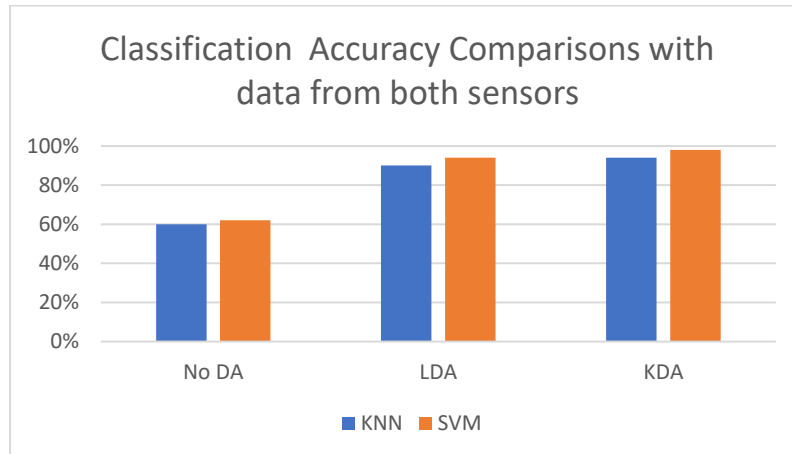


Figure 9. Driving activity classification accuracy for classifiers KNN and SVM for features extraction techniques on gyroscope and accelerometer data

## 5. Conclusion

In this paper, we have presented a model for detecting the maneuvering style of the driver which can help in identifying the culprit driver in case of a road side accident. The driver with the reckless or more aggressive driving style can be accounted for the accident. For our system, we have used an accelerometer and a gyroscope to collect data and apply features extraction and classification algorithm to identify the current driving activity and then based on the variance of values gathered from the gyroscope and accelerometer, categorized the driving style to be either, normal or reckless. We have used and evaluated features extraction algorithms, such as, linear discriminant



analysis and kernel discriminant analysis, and classification algorithms, such as, k-nearest neighbor and support vector machine to find the best possible solution for our model. According to the results, the combination of KDA and SVM provides the best accuracy for driving activity detection. In the future, we aim to explore other classification algorithms, such as, random forest, etc. to improve the efficiency of the system. We aim to implement another classifier for driving style categorization also.

Table 1. Threshold variance value for vehicle maneuvering-style detection

Driving Activity	Accuracy (Ac) & False Positive (FP) in percentages							
	Over-cautious		Normal		Aggressive		Reckless	
	Ac	FP	Ac	FP	Ac	FP	Ac	FP
Left-turn	70	30	96	4	98	2	99	0.5
Right-turn	70	30	96	4	98	2	99	0.5
Brake	78	22	99	0.5	99	0.5	99	0.5
Accelerate	65	35	95	5	97	3	99	1
Lane-change-left	60	40	90	10	95	5	99	1
Lane-change-right	60	40	90	10	95	5	99	1

## Acknowledgement

This work was supported by the Deanship of Research, Islamic University of Madinah, Kingdom of Saudi Arab [Project Title: “Automated Conflict Resolution for Car Accident Insurance Claims using Multi-Model Data Recording Device”, 24/39 ~ 1438-1439].

## 6. References

- [1] “Report: Saudi Arabia records 526,000 road accidents annually”, Saudi Gazette on Dec. 31, 2015, <http://english.alarabiya.net/en/News/middle-east/2016/01/01/Report-Saudi-Arabia-records-526-000-road-accidents-annually.html>
- [2] AM Al-Atwai and W Saleh, “Identification assessment and the enhancement of accident data collection and analysis in KSA” WIT Transactions on the Built Environment, Vol. 138, 2014

- [3] T. Nedal et al., “Characterization of crash-prone drivers in Saudi Arabia – A multivariate analysis”, *Case Studies on Transport Policy*, Volume 5, Issue 1, 2017, pp. 134-142
- [4] UB Gaffar, SM Ahmed, “A Review of Road traffic accident in Saudi Arabia: the neglected epidemic”, *Indian Journal of Forensic and Community Medicine*, 2015;2(4):242-246
- [5] “Traffic Accidents In The Kingdom By Region And Place Of Accident”, Ministry of Interior - General Directorate of Traffic, Saudi Open Data, <http://www.data.gov.sa/en/dataset/traffic-accidents>
- [6] “Driver Activity Recognition in identifying the Culprit for a Road Accident” has been published by the *International Journal of Research and Analytical Reviews (IJRAR)*, ISBN- 2349-5138 (print); 2348-1269 (online). IJAR August 2018, Volume 5, Issue 3, page no. 755-761
- [7] Khan, A.M.; Tufail, A.; Khattak, A.M.; Laine, T.H. Activity Recognition on Smartphones via Sensor-Fusion and KDA-Based SVMs. *Int. J. Distrib. Sens. Netw.* 2014, 2014, 1–14.
- [8] Thammasat, E.; Chaicharn, J. A simply fall-detection algorithm using accelerometers on a smartphone. *Proceedings of the Biomedical Engineering International Conference (BMEiCON)*, Ubon Ratchathani, Thailand, 5–7 December 2012.
- [9] Song, K.-T.; Wang, Y.Q. Remote activity monitoring of the elderly using a two-axis accelerometer. *Proceedings of the CACS Automatic Control Conference*, Tainan, Taiwan, November 18–19, 2005.
- [10] M. Mladenov, M. Mock, "A Step Counter Service for Java-Enabled Devices Using a Built-in Accelerometer", *Proc. 1st Int'l Workshop Context-Aware Middleware and Services (CAMS)*, pp. 1-5, 2009.
- [11] Hemminki, S.; Nurmi, P.; Tarkoma, S. Accelerometer-based Transportation Mode Detection on Smartphones. In *Proceedings of the 11th ACM Conference on Embedded Networked Sensor Systems (SenSys '13)*, Roma, Italy, 11–15 November 2013.
- [12] Cervantes-Villanueva, J.; Carrillo-Zapata, D.; Terroso-Saenz, F.; Valdes-Vela, M.; Skarmeta, A.F. Vehicle maneuver detection with accelerometer-based classification. *Sensors* 2016, 16, 1618.
- [13] Lara, O.D.; Labrador, M.A. A Survey on Human Activity Recognition using Wearable Sensors. *IEEE Commun. Surv. Tutor.* 2013, 15, 1192–1209.
- [14] Shoaib, M.; Bosch, S.; Incel, O.D.; Scholten, H.; Havinga, P.J. A survey of online activity recognition using mobile phones. *Sensors* 2015, 15, 2059–2085.
- [15] Attal, F.; Mohammed, S.; Dedabrishvili, M. Physical Human Activity Recognition Using Wearable Sensors. *Sensors* 2015, 15.
- [16] Preece, S.J.; Goulermas, J.Y.; Kenney, L.P.; Howard, D.; Meijer, K.; Crompton, R. Activity identification using body-mounted sensors—A review of classification techniques. *Physiol. Meas* 2009, 30, R1–R33

- [17] Wang, S.; Chen, C.; Ma, J. Accelerometer based transportation mode recognition on mobile phones. In Proceedings of the IEEE 2010 Asia-Pacific Conference on Wearable Computing Systems, Shenzhen, China, 17–18 April 2010; pp. 44–46.
- [18] Vaitkus, V.; Lengvenis, P.; Žylius, G. Driving style classification using long-term accelerometer information. In Proceedings of the 2014 19th International Conference On Methods and Models in Automation and Robotics (MMAR), Miedzyzdroje, Poland, 2–5 September 2014; pp. 641–644.
- [19] Dai, J.; Teng, J.; Bai, X.; Shen, Z.; Xuan, D. Mobile phone based drunk driving detection. In Proceedings of the 2010 4th International Conference on Pervasive Computing Technologies for Healthcare, London, UK, 1–3 April 2010; pp. 1–8.
- [20] Anguita, D.; Ghio, A.; Oneto, L.; Parra, X.; Reyes-Ortiz, J.L. Ambient Assisted Living and Home Care. In Human Activity Recognition on Smartphones Using a Multiclass Hardware-Friendly Support Vector Machine, Proceedings of the 4th International Workshop (IWAAL 2012), Vitoria-Gasteiz, Spain, 3–5 December 2012; Springer: Berlin/Heidelberg, Germany, 2012; pp. 216–223.
- [21] Thiemjarus, S.; Henpraserttae, A.; Marukatat, S. A study on instance-based learning with reduced training prototypes for device-context-independent activity recognition on a mobile phone. In Proceedings of the 2013 IEEE International Conference on Body Sensor Networks (BSN), Cambridge, MA, USA, 6–9 May 2013; pp. 1–6.
- [22] A.M. Khan, Y.-K. Lee, S.Y. Lee, and T.-S. Kim. Human activity recognition via an accelerometer enabled-smartphone using kernel discriminant analysis. In Proceedings of the 5th International Conference on Future Information Technology, pages 1–6, 2010
- [23] Abdi H, Williams LJ. Principal component analysis. *Wiley interdisciplinary reviews: computational statistics*. 2010 Jul;2(4):433-59.
- [24] Akaike, Hirotugu. "Fitting autoregressive models for prediction." *Annals of the institute of Statistical Mathematics* 21, no. 1 (1969): 243-247.
- [25] MotionNode Specification. [https://www.motionnode.com/MotionNode\\_Specification.pdf](https://www.motionnode.com/MotionNode_Specification.pdf), 2018 (accessed 20 December 2018).
- [26] Balakrishnama, Suresh, and Aravind Ganapathiraju. "Linear discriminant analysis-a brief tutorial." *Institute for Signal and information Processing* 18 (1998): 1-8.
- [27] Bianchi, Giovanni, and Roberto Sorrentino. *Electronic filter simulation & design*. McGraw Hill Professional, 2007.
- [28] Zhang, Yong, Junjie Li, Yaohua Guo, Chaonan Xu, Jie Bao, and Yunpeng Song. "Vehicle Driving Behavior Recognition Based on Multi-View Convolutional Neural Network (MV-CNN) with Joint Data Augmentation." *IEEE Transactions on Vehicular Technology* (2019).

- [29] World Health Organization (WHO): Global status report on road safety 2018, <https://apps.who.int/iris/bitstream/handle/10665/276462/9789241565684-eng.pdf?ua=1> (accessed on March 10<sup>th</sup>, 2019)
- [30] Aldegheishem, Abdulaziz, Humera Yasmeen, Hafsa Maryam, Munam Shah, Amjad Mehmood, Nabil Alrajeh, and Houbing Song. "Smart road traffic accidents reduction strategy based on intelligent transportation systems (tars)." *Sensors* 18, no. 7 (2018): 1983.